Advanced Ceramics Progress: Vol. 9, No. 4, (Autumn 2023) 22-31

Materials and Energy Research Center
MERC

Contents lists available at ACERP

Advanced Ceramics Progress

Journal Homepage: www.acerp.ir

Original Research Article

Experimental Investigation of the Effect of Reduced Graphene Oxide Addition on the Mechanical Properties and Behavior of Ti/RGO Composites in Spark Plasma Sintering Process with Reference to Potential Applications in Medical Implants

Syyed Mohammadreza Sedehi [a], Mohammadreza Maraki [b*], Seyed Davoud Houshyar Eftekhari [c], Mohammadreza Fazeli [a], Zahra Maleki [d], Fatemeh Norouzi Palangani [d]

[a] *Ph.D. Candidate, School of Mechanical Engineering, College of Engineering, University of Tehran, Tehran, Iran.*
[b] *Master, Department of Material Engineering, Birjand University of Technology, Birjand, Iran.*
[c] *Master, Department of Engineering, Islamic Azad University, Gonabad, Iran.*
[d] *Bachelor, Department of Engineering, Gonabad University, Gonabad, Iran.*

* Corresponding Author Email: Maraki@birjandut.ac.ir (Mohammadreza Maraki)
URL: https://www.acerp.ir/article_206327.html

ARTICLE INFO

Article History:

Received: 15 July 2024
Revised: 31 July 2024
Accepted: 07 September 2024

Keywords:

Titanium,
Reduced Graphene Oxide,
Spark Plasma Sintering,
Mechanical Properties,
Medical Implants

ABSTRACT

Given the strategic importance of pure titanium in sensitive industries, such as healthcare, and the existing weaknesses in the mechanical and physical properties of this metal, the present study aims to investigate the enhancement of its mechanical properties through the composite fabrication of pure titanium with Reduced Graphene Oxide (RGO) nanoparticles based on Spark Plasma Sintering (SPS) method. During the fabrication process, the mechanical properties of the samples were evaluated and compared using specialized tests. Composite fabrication is one of the effective and common methods for improving the material properties. As demonstrated in the results obtained in this study, the SPS method can be proposed as a reliable method for producing high-quality composites. Further evaluation of the mechanical properties of the samples reinforced with RGO indicates that the optimal presence of this reinforcement significantly enhances the mechanical properties compared to those of the pure samples. Moreover, the analysis of the behavior of the produced samples during the sintering process indicates a significant increase in the force and pressure in samples containing reduced graphene oxide, with no observed significant changes in displacement and temperature.

https://doi.org/10.30501/acp.2024.468057.1156

1. INTRODUCTION

As cases of tooth loss due to accidents continue to increase and population aging becomes a global issue, the demand for dental implant surgery is rising annually worldwide (Barootchi, S et al., 2020). To meet the rigid biological and mechanical requirements, dental implants must possess high strength, good corrosion resistance, and excellent biocompatibility. A variety of implant materials have been designed over the past decades, ranging from precious metals (Au, Pt, etc.) to stainless steel, CoCr alloys and titanium alloys, etc. Due to their relatively high strength, low density, low elastic

Please cite this article as: Sedehi, S. M., Maraki, M., Houshyar Eftekhari, S. D., Fazeli, M., Maleki, Z., Norouzi Palangani, F. "Experimental Investigation of the Effect of Reduced Graphene Oxide Addition on the Mechanical Properties and Behavior of Ti/RGO Composites in Spark Plasma Sintering Process with Reference to Potential Applications in Medical Implants", ***Advanced Ceramics Progress***, Vol. 9, No. 4, (2023), 22-31. https://doi.org/10.30501/acp.2024.468057.1156

modulus, and high corrosion resistance, titanium and its alloy have become popular dental implant materials among all metals (Pałka, K et al., 2018). To date, Ti and Ti alloys have been widely applied in dental implants. However, most of these implants rely on commercial pure Ti (cp-Ti), whose low strength (300 MPa) has greatly restricted its reliability in load-bearing implants such as dental screw etc., despite of its excellent biocompatibility and corrosion resistance (Niu, J et al., 2021). Some specific reinforcing particles such as TiB (Zhou, Z et al., 2023), TiC (Wang, J et al., 2024), SiC (Wang, L et al., 2024), ZrO_2 (Dwivedi, S et al., 2024), Al_2O_3 (Kaykilarli, C et al., 2024), and Y_2O_3 (Barootchi, S et al., 2020)have been introduced to improve the mechanical properties of titanium-based composites using different manufacturing technologies. Graphene and its allotropes are one of these materials. This valuable material, first synthesized by Andre Geim and Konstantin Novoselov in 2004 (Novoselov, K et al., 2004), can be used as a suitable reinforcement for composite materials due to its unique properties such as electrical (Schedin, F et al., 2007) , thermal properties (Balandin, A et al., 2008) , and tensile strength of 130 GPa (Lee, C et al., 2008) . In recent years, significant achievements have been made regarding the factors affecting the mechanical properties of titanium (Cao, H et al., 2020) , copper (Dong, L et al., 2017) , aluminum (Khodabakhshi, F et al., 2017) , and magnesium (Khodabakhshi, F et al., 2017) composites. Hang et al. (Cao, H et al., 2020) employed the same method and process of rolling during heat treatment to produce graphene-reinforced titanium composites and reported that increasing the sintering temperature from 600 to 900 C^O increases the density of composites from 84 up to 98 percent. In addition, the optimal solid-phase reaction temperature under the optimum spark plasma sintering parameters was 850 C^0, and the tensile strength could reach 1206 MPa for composites with a weight percentage of 0.3 after annealing and rolling at room temperature. Dong et al. (Dong, L. L et al., 2018) fabricated titanium-based composites with 0.6 wt% RGO using the spark plasma sintering method at temperatures ranging from 800 to 1100 C^O and studied the effects of sintering temperature on the microstructural changes and mechanical properties of the composites. They showed that the density of composites was improved upon increasing the sintering temperature. The optimal sintering temperature with a 5-minute duration under a pressure of 45 MPa was 1000 C^O, which created a good connection between the RGO reinforcement and the titanium matrix. Currently, skeletal bone diseases and related injuries have become more prevalent worldwide. Assessments have shown that over 50% of women and 20% of men over the age of 50 experience bone fractures during their remaining lifetime. Such bone defects may require surgery for complete knee and hip replacements or temporary and permanent implantation of components. This had led many researchers to pursue the development of a biological material that could mimic real bone properties such as flexibility and strength for repetitive use. Weihong Jin et al. (Jin, W et al., 2017)observed that medical materials cannot withstand loads in biological processes. Viktor Baltrus et al. referred to the significant role of these biological materials in the biological replacement of reconstructed alveolar bone insofar as some metals are now widely recognized as substitutes for natural bones. Over time, metallic materials lose their properties and fail to withstand pressure loads, thus making them susceptible to fractures. Additionally, metallic structures tend to weaken over time, leading to unintended effects such as toxicity and undesirable reactions. In the past two decades, implants for biomedical applications have undergone rapid and remarkable advancements. Titanium, due to the formation of a stable inert layer of titanium oxide on its surface, has superior biocompatibility compared to other metallic materials. With its low elastic modulus, lightweight, and reduced artifact production in computer tomography and magnetic resonance imaging compared to other metals, it has gained more popularity in the orthopedic field. Although Ti-6Al-4V is the most widely used titanium alloy for surgeries, despite its excellent performance and corrosion resistance, a high concentration of metal ions has been identified in the tissues surrounding the implants, questioning the long-term safety of the biological applications of this alloy. An alternative approach to overcoming the problem of harmful ion release is the application of pure titanium. However, the mechanical properties of commercial pure titanium are not as good as those of Ti64 alloy. In 2021, in one of the most interesting recent studies on graphene oxide-reinforced titanium-based composites, Sedehi et al. (Sedehi, S. M. R et al., 2021) successfully enhanced the mechanical properties and biocompatibility of commercial pure titanium through a combination of spark plasma sintering composite fabrication and severe plastic deformation methods. Despite the fact that relatively limited information is available on the effect of reduced graphene oxide presence on the behavior of titanium-based composites during spark plasma sintering, it has been established that the presence of this type of nanoparticles significantly contributes to the enhancement of composite properties. This research primarily aims to investigate these behaviors in titanium-based composites reinforced with different percentages of RGO during spark plasma sintering.

2. MATERIALS AND METHODS

The reduced graphene oxide was prepared from Nano part Aseman Company in Gonabad County. Spherical pure titanium powder, with the features given in Table 1, was also used as the primary material in this study. To

achieve an optimal and uniform composite structure, the following four stages were followed based on powder metallurgy principles: a) Initially, RGO nanosheets with the weight percentages of 0.05% and 0.1% were added to pure ethanol and sonicated until a dark and homogeneous solution was obtained. This physical property indicates that RGO is fully dispersed in ethanol. b) Pure titanium powder was also mixed with ethanol and vigorously stirred at room temperature. Then, both solutions were mixed for 30 min to achieve a homogeneous slurry. c) The mixed slurry was completely dried using a vacuum furnace and then ball-milled under argon gas protection for 5 h at the speed of 350 rpm with a powder-to-ball ratio of 1:10 (zirconia balls). d) The prepared powders in the previous stages were loaded into graphite molds with an inner diameter of 25 mm and a height of 50 mm and then, they were subjected to spark plasma sintering at the temperature of 900 C° and pressure of 45 MPa. The displacement rate during the sintering process is described as follws (Sugita, T et al., 1970):

$$\varepsilon = \frac{d\varepsilon}{dt} = A\,\frac{\varphi\mu b}{KT}\left(\frac{b}{G}\right)^{p}\left(\frac{\sigma}{\mu}\right)^{n} \quad (1)$$

where ε is the displacement rate, t the time (sec), A the constant coefficient, φ the diffusion coefficient, μ the shear modulus, b the Burgers vector, K the Boltzmann constant (1.38×10^{-23} j/K), T the sintering temperature (Kelvin), G the grain size (nm), σ the microscopic stress (MPa), P the grain growth rate, and n the effective stress. Generally, material displacement during spark plasma sintering process is directly proportional to the sintering time at high temperatures. In this regard, the kinetic equation of the process can be written as (Ting, C et al., 1999) :

$$\frac{1}{D}\frac{dD}{dt} = \frac{B\varphi\mu_{eff}b}{KT}\left(\frac{b}{G}\right)^{p}\left(\frac{\sigma_{eff}}{\mu_{eff}}\right)^{n} \quad (2)$$

where D denotes the relative density percentage, B a constant coefficient, σ the instantaneous compressive stress (MPa), and μeff the instantaneous shear stress (MPa). As described by Ashbi (Chaim, R et al., 2010) , the applied pressure is determined based on Formula 3:

$$\sigma_{eff} = \frac{1-D}{(D-D_0)D^2}\,\sigma_{mac} \quad (3)$$

where σ mac = 45 MPa and D_0 represent the initial relative density (40%). The Young's modulus of the porous material can also be calculated through the following equation [23]:

$$\frac{E_{eff}}{E_{th}} = 1 - \frac{P}{P_0} \quad (4)$$

where E_{eff} represent the effective Young's modulus (GPa), E_{th} the Young's modulus of the compacted material (gigapascals), p = 1-D the actual porosity, and P_0 = 1-D_0 the initial porosity (percentage). Here, μeff can be expressed using Equation 5 (Dong, L. L et al., 2018):

$$\mu_{eff} = \frac{E_{eff}}{2(1-V_{eff})} \quad (5)$$

The kinetic equations of the spark plasma sintering process can also be expressed as follows [23]:

$$\frac{1}{\mu_{eff}}\frac{1}{D}\frac{dD}{dt} = K\,\frac{\frac{Q_d}{Rt}}{T}\left(\frac{b}{G}\right)^{p}\left(\frac{\sigma_{eff}}{\mu_{eff}}\right)^{n} \quad (6)$$

$$\mathrm{Ln}\left(\frac{1}{\mu_{eff}}\frac{1}{D}\frac{dD}{dt}\right) = n\ln\left(\frac{\sigma_{eff}}{\mu_{eff}}\right) + K_1 \quad (7)$$

where K is the constant coefficient, R the gas constant (8.314 J/(mol.K)), and Qd the activation energy for surface diffusion (joules). Therefore, the above equation can be rewritten as Y = nX + K1. Based on the results from the previous research studies [5] as well as the equations provided, the optimal sintering temperature for titanium is chosen to be between 900 to 1000 C°. In the following, for more convenience, the experimental samples are labeled as follows: pure sintered sample, sintered sample containing 0.5% weight fraction RGO, and sintered sample containing 1.0% weight fraction RGO. The experimental procedures are illustrated in Fig.1.

TABLE 1. Specifications of RGO powder

Purity (%)	Aver. part. size (lm)	True density (g/cm³)	Volatile (%)	Ash (%)
99/28	4/81	2/23	0/67	0/05

TABLE 2. Specifications of the Ti powder used

Powder	Impurity content (mass%)					Density (g/cm³)	Particle size (μm)
Ti	O	Fe	N	C	Si	4/51	45
	0/27	0/05	0/03	0/02	0/02		

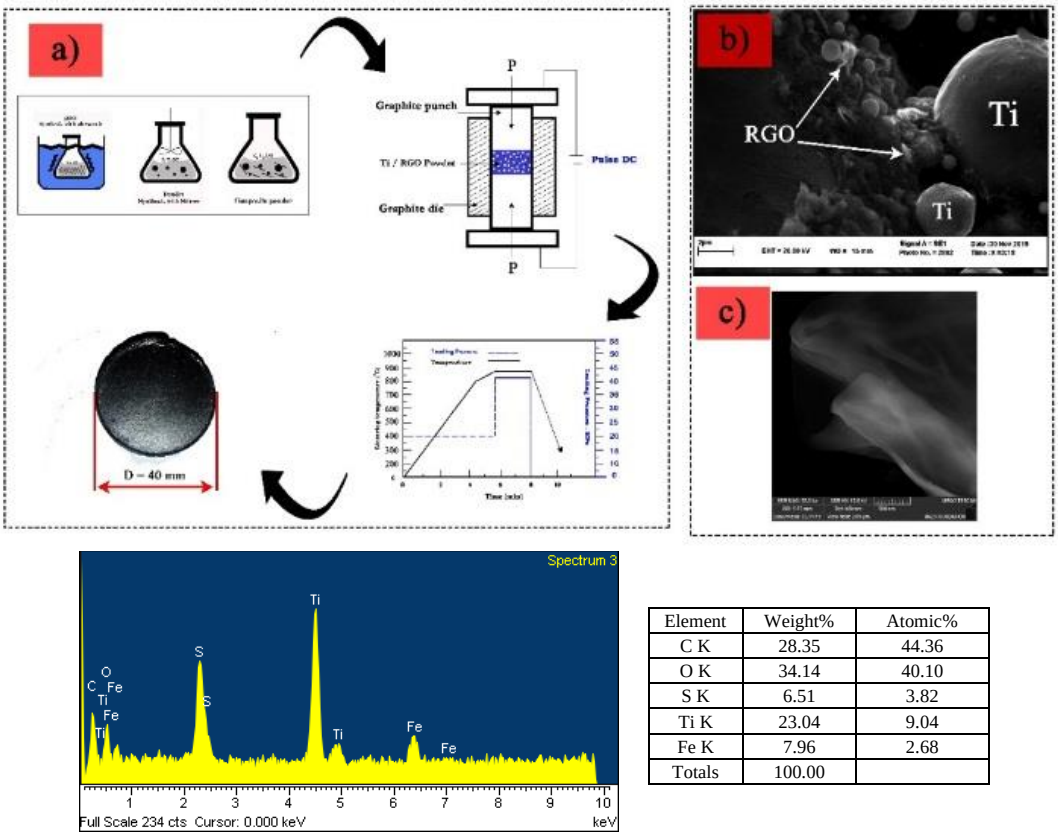

Element	Weight%	Atomic%
C K	28.35	44.36
O K	34.14	40.10
S K	6.51	3.82
Ti K	23.04	9.04
Fe K	7.96	2.68
Totals	100.00	

Figure 1. a) Schematic of the fabrication cycle, b, c) SEM images of the produced composite and RGO.

Characterization

To further investigate the existing phases and determine the presence and nature of RGO in the composite, X-Ray Diffraction (XRD) was conducted using an Explorer device manufactured by GNR Italy. In addition, to examine the morphological changes of the initial powders and produced samples, a Field Emission Scanning Electron Microscope (SEM) model MIRA3 from TESCAN, Czech Republic, with a resolution capability down to 1.5 nm at 15 kilovolts voltage, was employed. Further, the hardness of the samples was measured using a Vickers hardness tester model KOOPA-UV1 under a load of 30 kg at the dwell time of 10 sec. To obtain the average value, at least 3 repetitions of the hardness test were performed for each sample, and the Vickers microhardness value was calculated using the following equation:

$$HV = 1/8544 \frac{P}{d^2}$$

The tensile test was also conducted using an MTS810 testing machine at the speed of 1 mm/min at room temperature (ASTM E8M/E8-16a).

3. Results and discussion

Hardness

Incorporation of RGO into titanium matrix composites and application of Spark Plasma Sintering (SPS) can significantly enhance the hardness of these materials. RGO, with its two-dimensional structure and strong carbon-carbon bonds, acts as an excellent reinforcing material. When RGO is incorporated into the titanium matrix, its sheets are uniformly distributed that prevents dislocation motion and crack propagation, thereby increasing the overall hardness of the composite. The strong bonds formed between RGO and titanium particles also facilitate effective load transfer. The SPS method, due to its short processing time and relatively low temperatures, ensures uniform distribution of RGO and reduces the likelihood of defect and internal void formation. This method employs rapid electrical pulses to compress and sinter the powders at lower temperatures, compared to traditional methods, reducing the grain growth, maintaining fine grain sizes, and ultimately contributing to enhanced hardness. Such enhanced hardness of titanium composites resulting from addition of RGO and implementation of the SPS method can have a significant impact on improving the mechanical properties of the medical implants. Titanium implants are widely used in the medical field due to their excellent mechanical properties and biocompatibility, yet there is a need to improve their hardness and wear

resistance to increase their longevity and performance. Incorporating RGO into the titanium composites not only enhances the hardness but also improves the fatigue and wear resistance of the implants. Owing to these features, the RGO-reinforced titanium implants become more durable and exhibit a better performance in the body, which is particularly of high importance in orthopedic and dental applications. The results of Vickers microhardness tests on the specimens at various stages are shown in Fig.2.

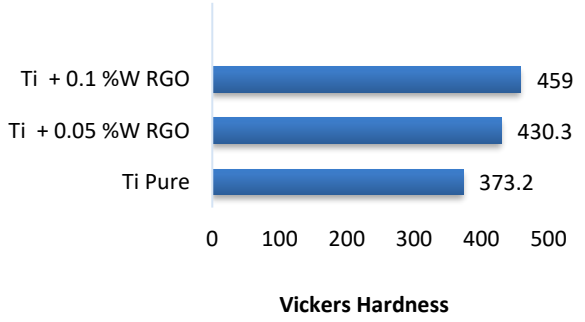

Figure 2. Hardness results

XRD

The figure below shows the X-Ray Diffraction (XRD) spectrum under the conditions of V=40 kV, Current=30 mA, and Detector type: Dectris. Evidently, titanium (Ti) and titanium carbide (TiC) phases are the main phases in the composite, whose peaks correspond to pure titanium powder serving as a reference; hence, the peak at 40 degrees is considered the strongest peak present in titanium. Additionally, weaker peaks are identified at the angles 34, 38, 53, 63, 71, 77, and 78 degrees. The Ti phase alone can only be observed in the pure titanium sample. The weak peak labeled (002) at an angle of 5.26° is attributed to the reduced graphene oxide. This peak is exclusive to components containing RGO. Changes in the intensity and position of the peaks are also observed in subsequent stages of the experiment, with the most significant peaks attributed to TiC at 43 degrees during the sintering stage. As a result of using a graphite mold and carbon infiltration, the formation of the TiC phase is observed in both pure and RGO-containing samples. The intensity of the TiC phase increases with an increase in the sintering time and temperature, which has been reported in previous studies when the sintering temperature exceeds 800 C^O [19]. The standard Gibbs free energy (ΔG) of TiC formation from the reaction between Ti and carbon can be expressed as (Sedehi, S. M. R et al., 2021) :

$\triangle G = -184571.8 + 41.382T \ -5.042TlnT + 2.425 \times 10\text{-}3T2 - 9.79 \times 105/T$ (T＜1939 K)

where ΔG represents the Gibbs free energy in kilojoules per mole, and T the reaction temperature in Kelvin. Given the sintering temperature of 900 C^O in this study, it can be concluded that TiC particles were formed during the spark plasma sintering process, as shown below (Sedehi, S. M. R et al., 2021) :

$\triangle G = -184571.8 + 41.382(1173.15) - 5.042(1173.15)\ln(1173.15) + 2.425 \times 10\text{-}3(1173.15)2 - 9.79 \times 105/(1173.15) = -175325.641$

Therefore, all processes proved to be ideally controlled in terms of phase control, hence successful. To provide further details on carbon atom diffusion within the composite, the depth profile of carbon penetration is shown in Fig. 3. As evident in this figure, at point 6, which is close to the surface, the carbon content was approximately 19.62% by weight that decreased towards the center of the sample. In this regard, the carbon content at point 5 was found to be approximately 5.5% by weight. As mentioned earlier, the carbon content may increase as a result of the formation of the TiC phase. The formation of the TiC (titanium carbide) phase in the titanium-based composites can significantly impact the mechanical properties and performance of medical implants. TiC, known for its high hardness, wear resistance, and chemical stability, acts as a reinforcing phase within the titanium matrix. Adding TiC to titanium can enhance the hardness and wear resistance of the medical implants, thereby improving their longevity and performance, since implants are prone to severe mechanical forces and wear within the body. Additionally, the TiC phase, due to its integration with the titanium matrix, can improve the thermal properties of implants and reduce their thermal expansion, which is crucial under the varying environmental conditions within the body. Although the presence of this phase has not been specifically and fully validated for medical applications, it has gained significance through research on in vivo implants, hence considered a safe material for this field (Gonçalves, V. R. M et al., 2024) . Further, higher degrees of hardness and wear-resistance of the TiC surface decrease the amount of wear particles released from the implant surface, which in turn leads to inflammatory responses and long-term complications within the body. Consequently, the formation of the TiC phase in the titanium-based implants can significantly enhance their mechanical and biological performance, increasing their lifespan and efficacy in medical applications.

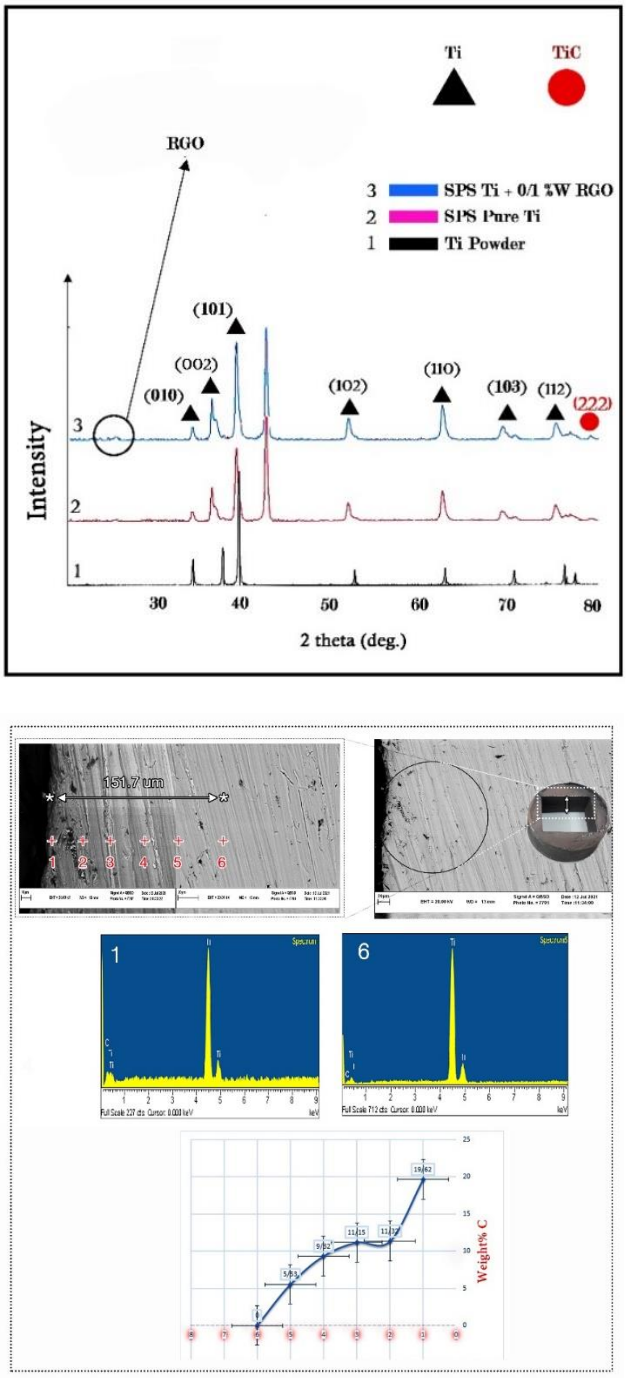

Figure 3. XRD Results and Carbon Penetration in the Composite after SPS Process

Tensile strength

Fig.4 presents the results of the tensile strength for Ti/RGO composite at different percentages of RGO, compared to the pure sample. As expected, compared to the pure sample, the samples containing graphene in the plasma sintering stage showed an optimal increase in their strength, indicating uniform distribution of the reinforcement particles. However, in the third sample with the highest amount of RGO, a suitable bond between titanium particles and RGO nanoparticles has not been established, hence a decrease in strength compared to the second sample. At this stage, the tensile strengths of the samples are recorded as 670.19, 824.71, and 821.42 MPa, respectively, and the yield strengths are calculated as 660, 800, and 780 MPa, respectively. According to the obtained results, compared to the pure sample, the tensile and yield strength values showed a significantly optimal growth upon increasing weight percentage of RGO.

Additionally, in Figure 5a-b, fractography images of the fracture surfaces of the tensile test specimens are displayed, indicating that the fracture surface of the pure sample has broader cracks than those in the sample containing RGO, hence the smaller crack widths. This factor could serve as evidence for the increased tensile strength of the reinforced samples. The fractographic analysis of the Ti/RGO composite indicates that the presence of the RGO nanoparticles significantly impacts the mechanical behavior and fracture characteristics of the material. Firstly, RGO ensures uniform stress distribution within the titanium matrix, preventing stress concentration at specific points and thereby reducing crack width. Secondly, these nanoparticles form stronger bonds between titanium particles, inhibiting rapid crack propagation. Additionally, RGO acts as a physical barrier along the crack propagation path, deflecting and slowing down crack growth, which further reduces crack width. Finally, the presence of RGO enhances energy absorption during fracture, leading to finer cracks with smaller widths. Collectively, these factors contribute to improved mechanical behavior, increased tensile strength, and enhanced fracture resistance of the Ti/RGO composite compared to the pure sample.

For instance, in knee implants requiring high resistance to mechanical pressures and tensile strength, the presence of smaller and finer cracks in RGO-containing samples can promote more uniform stress distribution within the titanium matrix, mitigating stress concentrations at specific points. This property may reduce susceptibility to failure and enhance the lifespan of knee implants. Similarly, in dental implants where seamless integration with surrounding natural tissues is crucial, the presence of fewer and finer cracks in RGO-containing samples can potentially reduce bacterial invasion risks and maintain surface integrity. Overall, these analyses demonstrate that inclusion of RGO nanoparticles can improve the mechanical behavior and fracture resistance of Ti/RGO implants compared to pure titanium samples.

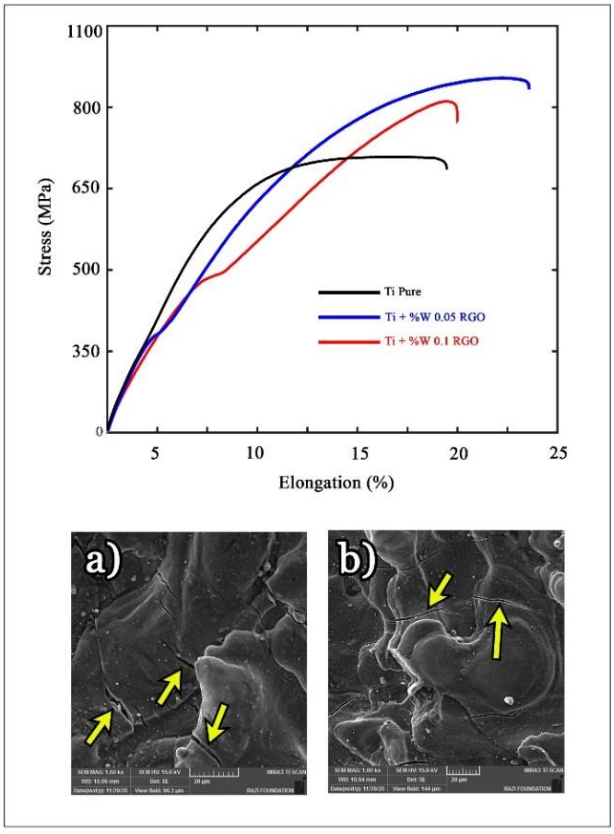

Figure 4. Tensile Test Results and Fractography Images a) Pure Sample b) Sample Containing RGO

Analysis of the Behavior of Produced Samples Based on the Output Variables of the SPS Device during the Fabrication Process

In previous research with a main focus on the implementation of spark plasma sintering for composite fabrication, little attention has been paid to the outputs of the device as well as the behavior of the produced composites during the process. Given the high importance of analyzing the behavior of RGO-reinforced composites, this study focused on the behavior of the pure and RGO-reinforced samples at different percentages of RGO during the process, yielding

interesting results. Fig.5 illustrates the displacement, force, pressure, and temperature of the three produced samples in this study: the first sample was pure titanium, and the next two samples contained RGO with different percentages. As observed in this figure, no significant changes were observed in the displacement parameter for the three produced samples. However, in terms of force and pressure, it is quite evident that while the pure titanium sample undergoes a descending trend during the process, the other two samples containing RGO possess an optimum level of force and pressure during the process. To be specific, the force imposed on the pure titanium sample reached its minimum level of 1450 N, while that on the second and third samples reached 1850 and 1780 N, respectively. Similarly, the minimum pressure before loading completion for the three samples was 29, 37, and 36 MPa, respectively, indicating the significance of analyzing the output parameters of the behavior of the produced composite with the SPS method. The temperature variable was also recorded continuously during the process using sensors embedded in the device and mold. However, no significant changes were observed in temperature for these three samples throughout the process. In summary, the output results from the device regarding the analysis of the behavior of the produced samples show that the recorded force and pressure are consistent with the results from the tensile test. It can be concluded that although the presence of RGO increases the force and pressure imposed on the mold during the process, the good connection between the matrix and reinforcement achieved after sintering has also increased the tensile strength and yield strength of the samples.

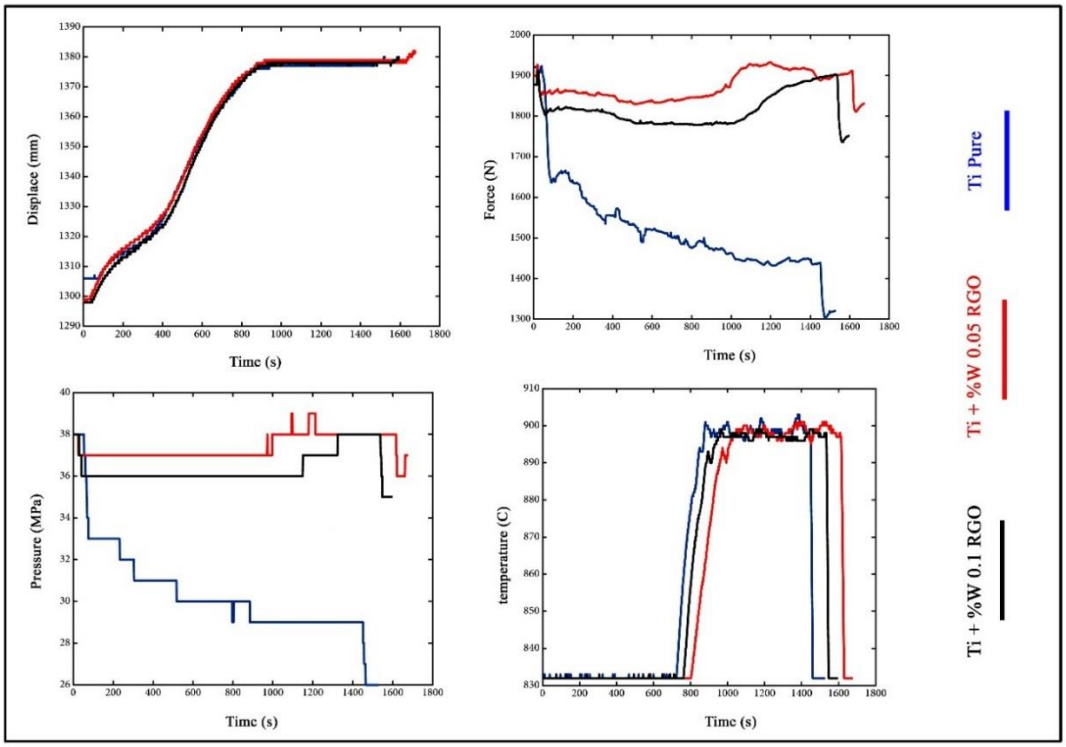

Figure 5. Behavior of different produced samples using output variables during the SPS process

Conclusions

Composite synthesis method is a common and effective method for enhancing various properties. In this study, titanium samples reinforced with reduced graphene oxide nanoparticles were fabricated using spark plasma sintering method at the temperature of 900 C°, pressure of 45 MPa, and time of 6 min. The effect of RGO presence on the mechanical properties and behavior of the samples during the sintering process was investigated, and the following conclusions were drawn

1. Based on the summary of the research results, Spark Plasma Sintering (SPS) method was proposed introduced as a reliable technique for producing high-quality composites. However, due to the sensitivity of the method to phase formation, it may adversely affect the quality of produced components, especially in certain medical applications. Additionally, unlike conventional manufacturing processes, the SPS method had some limitations in the size and complexity of parts it produced. Considering these advantages and disadvantages, application of SPS for titanium component production for medical applications required precise evaluation and thorough understanding of the properties and requirements of the intended products to achieve the optimal outcomes and efficiency.

2. The formation of the TiC (titanium carbide) phase in titanium-based composites could significantly affect the mechanical properties and performance of medical implants due to its high hardness, wear resistance, and chemical stability. Additionally, once integrated with the titanium matrix, the TiC phase enhanced the thermal properties of implants and reduced their thermal expansion, which is crucial under the variable environmental conditions within the body.
3. The results of the mechanical properties of RGO-reinforced samples indicated that although the presence of this reinforcement increases the mechanical properties compared to the pure sample, a diminishing return trend was observed among the samples with different RGO concentrations.
4. The analysis of the behavior of the produced samples during the sintering process, conducted using precise sensors installed in the device and mold, indicates that in samples containing RGO, the force and pressure increase significantly and maintain a relatively constant level, whereas in the pure sample, a noticeable descending trend is experienced.
5. Regarding the output values of the samples' behavior during the process, displacement and temperature did not show specific sensitivity to the presence of graphene, and all three samples exhibited similar behavior.

Acknowledgments

The authors would like to express their appreciation to Nano Part Aseman Company in Gonabad County for providing the raw materials, as well as Bargaz (https://bargaz.ir/) and Kohmax companies (https://koohmax.ir/) in Gonabad County for their constructive support, which has greatly benefited them.

References

1. Balandin, A. A., Ghosh, S., Bao, W., Calizo, I., Teweldebrhan, D., Miao, F., & Lau, C. N. (2008). Superior thermal conductivity of single-layer graphene. Nano letters, 8(3), 902-907. https://doi.org/10.1021/nl0731872.
2. Barootchi, S., Chan, H. L., Namazi, S. S., Wang, H. L., & Kripfgans, O. D. (2020). Ultrasonographic characterization of lingual structures pertinent to oral, periodontal, and implant surgery. Clinical oral implants research, 31(4), 352-359. https://doi.org/10.1111/clr.13573
3. Cao, H. C., & Liang, Y. L. (2020). The microstructures and mechanical properties of graphene-reinforced titanium matrix composites. Journal of Alloys and Compounds, 812, 152057. https://doi.org/ 10.1016/j.jallcom.2019.152057.
4. Chaim, R., & Bar-Hama, O. R. (2010). Densification of nanocrystalline NiO ceramics by spark plasma sintering. Materials Science and Engineering: A, 527(3), 462-468. https://doi.org/10.1016/j. msea.2009.10.011.
5. Dang, Q., Huang, G., Wang, Y., Zhang, C., Liu, G. H., & Wang, Z. D. (2024). Mechanical properties and thermal deformation behavior of low-cost titanium matrix composites prepared by a structure-optimized Y2O3 crucible. Journal of Iron and Steel Research International, 31(3), 738-751. https://link.springer.com/article/10.1007/s42243-023-01093-2.
6. Dong, L., Chen, W., Deng, N., Song, J., & Wang, J. (2017). Investigation on arc erosion behaviors and mechanism of W70Cu30 electrical contact materials adding graphene. Journal of Alloys and Compounds, 696, 923-930. https://doi.org/10.1016/j.jallcom.2016.12.044.
7. Dong, L. L., Xiao, B., Liu, Y., Li, Y. L., Fu, Y. Q., Zhao, Y. Q., & Zhang, Y. S. (2018). Sintering effect on microstructural evolution and mechanical properties of spark plasma sintered Ti matrix composites reinforced by reduced graphene oxides. Ceramics International, 44(15), 17835-17844. https://doi.org/10.1016/j.ceramint.2018.06.252.
8. Dwivedi, S. P., Saxena, K. K., Sharma, S., & Chaudhary, V. (2024). Effect of Yttria-Stabilized Zirconia addition along with Cu in development of titanium based metal matrix composite via FSP technique for the application in biomedical devices. Composite Interfaces, 1-25. https://doi.org/10.1080/09276440.2024.2330789
9. Gonçalves, V. R. M., Corrêa, D. R. N., de Sousa, T. D. S. P., Pintão, C. A. F., Grandini, C. R., Afonso, C. R. M., & Lisboa-Filho, P. N. (2024). Promising composites for wear resistant load-bearing implant applications: Low elastic moduli of β Ti–Nb alloy reinforced with TiC particles and/or TiB whiskers. Journal of Materials Research and Technology, 30, 879-889. https://www.sciencedirect.com/science/article/pii/S2238785424006641.
10. Jin, W., & Chu, P. K. "Orthopedic implants," Vol. 17, No.20, pp. 1- 15, 2017. http://www.google.com/url?sa=t&rct=j&q=&esrc=s&source=web&cd=&cad=rja&uact=8&ved=2ahUKEwj6h6jsqNuIAxVBgf0HHYMFCaYQFnoECBAQAQ&url=http%3A%2F%2Fwww.cityu.edu.hk%2Fphy%2Fappkchu%2FPublications%2F2019%2F19.04.pdf&usg=AOvVaw1O25mAKDgX-pRSAGJfX6ly&opi=89978449
11. Kaykilarli, C., Uzunsoy, D., & Yeprem, H. A. (2024). Role of process control agent in the production of Al2O3-reinforced titanium matrix composites. Ceramics International, 50(9), 16452-16462. https://www.sciencedirect.com/science/article/pii/S0272884224006266.
12. Khodabakhshi, F., Arab, S. M., Švec, P., & Gerlich, A. P. (2017). Fabrication of a new Al-Mg/graphene nanocomposite by multi-pass friction-stir processing: dispersion, microstructure, stability, and strengthening. Materials Characterization, 132, 92-107. https://doi.org/ 10.1016/j.matchar.2017.08.009.
13. Lee, C., Wei, X., Kysar, J. W., & Hone, J. (2008). Measurement of the elastic properties and intrinsic strength of monolayer graphene. Science, 321(5887), 385-388. https://doi.org/10.1126/science.1157996.
14. Niu, J., Guo, Y., Li, K., Liu, W., Dan, Z., Sun, Z., ... & Zhou, L. (2021). Improved mechanical, bio-corrosion properties and in vitro cell responses of Ti-Fe alloys as candidate dental implants. Materials Science and Engineering: C, 122, 111917. https://www.sciencedirect.com/science/article/pii/S0928493121000552.
15. Novoselov, K. S., Geim, A. K., Morozov, S. V., Jiang, D. E., Zhang, Y., Dubonos, S. V., ... & Firsov, A. A. (2004). Electric field effect in atomically thin carbon films. Science, 306(5696), 666-669. https://www.science.org/doi/abs/10.1126/science.1102896.
16. Pałka, K., & Pokrowiecki, R. (2018). Porous titanium implants: a review. Advanced Engineering Materials, 20(5), 1700648. https://doi.org/10.1002/adem.201700648
17. Schedin, F., Geim, A. K., Morozov, S. V., Hill, E. W., Blake, P., Katsnelson, M. I., & Novoselov, K. S. (2007). Detection of individual gas molecules adsorbed on graphene. Nature materials, 6(9), 652-655. https://doi.org/10.1038/nmat1967.

18. Sedehi, S. M. R., Khosravi, M., & Yaghoubinezhad, Y. (2021). Mechanical properties and microstructures of reduced graphene oxide reinforced titanium matrix composites produced by spark plasma sintering and simple shear extrusion. Ceramics International, 47(23), 33180-33190. https://www.sciencedirect.com/science/article/pii/S0272884221026195.

19. Sugita, T., & PASK, J. A. (1970). Creep of doped polycrystalline Al2O3. Journal of the American Ceramic Society, 53(11), 609-613. https://doi.org/10.1111/j.1151-2916.1970.tb15983.x.

20. Ting, C. J., & Lu, H. Y. (1999). Hot-pressing of magnesium aluminate spinel—I. Kinetics and densification mechanism. Acta materialia, 47(3), 817-830. https://doi.org/10.1016/S1359-6454(98)00400-5.

21. Wang, J., Tang, L., Xue, Y., Zhao, Z., Ye, Z., Cao, W., ... & Jiang, F. (2024). Microstructure and properties of (diamond+ TiC) reinforced Ti6Al4V titanium matrix composites manufactured by directed energy deposition. Journal of Materials Research and Technology, 28, 3110-3120. https://www.sciencedirect.com/science/article/pii/S223878542303291X.

22. Wang, L., Yuan, S., Gao, X., Li, Q., Xu, W., An, W., ... & Chen, B. (2024). Unveiling Damage Mechanisms of SiC Fiber-reinforced Titanium Matrix Composites through Ultrasonic Scratching. Journal of Cleaner Production, 142820. https://www.sciencedirect.com/science/article/pii/S0959652624022698.

23. Zhou, Z., & Liu, Y. (2023). New insights into the evolution of TiB whisker and TiC particle during selective laser melting of titanium matrix composites. Materials Science and Engineering: A, 877, 145200. https://www.sciencedirect.com/science/article/pii/S092150932300624X.